

# Magnetic Properties of Nickel Ferrite Nanoparticles Prepared Using Flotation Extraction

Yu. A. Mirgorod<sup>a</sup>, N. A. Borshch<sup>a</sup>, V. M. Fedosyuk<sup>b</sup>, and G. Yu. Yurkov<sup>c</sup>

<sup>a</sup> Southwest State University, ul. 50 let Oktyabrya 94, Kursk, 305040 Russia

<sup>b</sup> Scientific-Practical Materials Research Centre, Belarussian Academy of Sciences, ul. Brovki 19, Minsk, 220072 Belarus

<sup>c</sup> Baikov Institute of Metallurgy and Materials Science, Russian Academy of Sciences, Leninskii pr. 49, Moscow, 119991 Russia

e-mail: yu\_mirgorod@mail.ru

Received May 2, 2012

**Abstract**—A method has been proposed for the preparation of nickel ferrite nanoparticles in a system of direct sodium dodecyl sulfate micelles using ion flotation. Amorphous nickel ferrite nanoparticles with the overall composition  $x\text{NiFe}_2\text{O}_4 \cdot y\text{Fe}_2\text{O}_3 \cdot z\text{H}_2\text{O}$ , containing dodecyl sulfate anion impurities, have been prepared. According to transmission electron microscopy results, the size distribution of the synthesized nanoparticles has a maximum in the range 4 to 6 nm, and the ferrite is X-ray amorphous. The blocking temperature of the synthesized nanoparticles is 25 K. The ferrite possesses superparamagnetic properties, with a specific saturation magnetization of 15 A m<sup>2</sup>/kg at 5 K.

**DOI:** 10.1134/S0020168512110064

## INTRODUCTION

Nanoparticles of the  $\text{MFe}_2\text{O}_4$  ( $\text{M} = \text{Ni, Co, Mn, Zn}$ ) transition metal ferrites are used in the fabrication of magnetic fluids, magnetic information carriers, and microwave radiation shields [1, 2]. Nickel ferrite nanoparticles have high permeability at high frequencies and high electrical conductivity [3]. They are also used as contrast agents in magnetic resonance imaging [4], anode materials for lithium ion batteries [5], and catalysts for the preparation of halogen derivatives of aromatic hydrocarbons [6]. Organic coatings reduce the magnetization of nickel ferrite nanoparticles [7]. The electrical resistance of nanoporous and thin-film nickel ferrite decreases upon the adsorption of chlorine [8], hydrocarbons [9], ethanol [10], and other substances [11].

Nickel ferrite nanocrystals can be prepared using hydrothermal processing [12], ball milling [13], combustion reactions [14], and reverse micelles [15]. Synthesis in reverse micelles is carried out in a water-amphiphile-hydrocarbon three-component solution with a limited number of amphiphiles. Use is commonly made of sodium bis(2-ethylhexyl) sulfosuccinate, which has an optimal hydrophilic-lipophilic balance for the formation of reverse micelles.

In this report, we propose a hybrid process for the preparation of ferrite nanoparticles from used magnetic materials. The process includes the preconcentration of simple or complex metal ions in the course of ion flotation [15] as its first step, followed by the synthesis of nanoparticles from the resultant precursors in a system of direct micelles as its second step [16]. The flotation extraction process requires relatively little energy and can be used in the case of large volumes of dilute aque-

ous solutions. After flotation extraction, the amphiphiles are used in the synthesis of nanoparticles in direct micelles. In the synthesis of ferrites, one can use anionic amphiphiles of various structures, forming micelles in an aqueous solution. Used magnetic materials are dissolved in acids. Flotation extraction is applicable in both large- and small-scale manufacture, with the use of simple flotation machines.

## EXPERIMENTAL

In this study, nickel ferrite was synthesized by the following procedure: Sodium dodecyl sulfate (SDS) (Shostka Chemical Reagents Plant) was recrystallized from water and ethanol. The purity of amphiphiles was ascertained from the lack of a minimum in the surface tension isotherm of their aqueous solutions near the critical micelle concentration (CMC),  $8 \times 10^{-3}$  M. Surface tension was measured by the Wilhelmy plate method with an accuracy of  $\pm 0.1$  mN/m.

Nickel ferrite nanoparticles were prepared using reagent-grade iron(II) sulfate ( $\text{FeSO}_4 \cdot 6\text{H}_2\text{O}$ ) and nickel chloride ( $\text{NiCl}_2 \cdot 6\text{H}_2\text{O}$ ). The organic phase used in flotation extraction was a mixture of toluene and isoamyl alcohol in the volume ratio 4 : 1 (Fluka reagents).

The flotation extraction process was run in a purpose-designed 2-L reactor. Its bottom part had a ceramic distributor for air delivery through a rotameter with the use of a compressor. The air distributor was secured so that it could be withdrawn in order to purify the column. The air introduced into the column was broken down into bubbles, which transferred SDS and metal ions on their surface to an extractant, situated on the surface of an aqueous solution in the form of a sep-

Quantitative elemental analysis data for the synthesized powder

Element	Energy, keV	Weight percent	Atomic percent	Uncertainty, %
O	0.525	41.93	70.68	0.30
C	1.739	3.19	3.06	0.42
Fe	6.398	44.57	21.52	0.94
Ni	7.471	10.31	4.73	1.57

arate phase, which was released from the top part of the column through an access hole. The compressor was connected to the column by rubber tubes. Glass stop-cocks were used to control the air flow rate and the column discharge flow rate.

The synthesis of nickel ferrite nanoparticles through the flotation extraction of precursors with SDS was tested using model solutions. The  $\text{NiCl}_2$  and  $\text{FeSO}_4$  concentrations in solution were  $1 \times 10^{-4}$  M. To 1500 mL of solution was added SDS to give a concentration of  $4 \times 10^{-4}$  M. The SDS was dissolved in 5 mL of ethanol and only then added to an aqueous solution in order to avoid untimely formation of micelles, which otherwise might have prevented the preparation of nickel and iron dodecyl sulfates. The metal ions were floated for 10 min. As a result, the solution became colorless and the organic phase turned green, indicating that the nickel ions were transferred from one phase to another. After the flotation extraction process, the extractant and precursor were separated from the aqueous solution. The solvent was distilled off and the residue was vacuum-dried in order to remove the toluene and isoamyl alcohol. The resultant powder was dissolved in distilled water to the critical micelle concentration of the salts obtained and was treated with sodium hydroxide until the complete precipitation of iron and nickel hydroxides. This was accompanied by partial reduction of the nickel hydroxide because of its amphoteric nature, which eventually led to the formation of a "magnetic colloid," consisting of X-ray amorphous nonstoichiometric nickel ferrite and an iron oxide.

The precipitate was filtered off, and the resultant powder was dried in air for several days and then in a drying chamber at 50°C for 3 h. This powder preparation procedure, with no calcination, was used in order to preserve the amphiphiles that formed a protective adlayer on the powder nanoparticles and thus prevented them from sticking together.

X-ray diffraction (XRD) patterns of the powder thus prepared were collected on a DRON-3M diffractometer using a copper target X-ray tube. In addition, an XRD pattern was calculated for a cubic lattice parameter of  $\text{Fe}_3\text{O}_4$ ,  $a = 0.838$  nm, taken from a crystallographic database and the Fe ions on the A site of the spinel structure replaced by nickel ions. The calculated XRD pattern of such an inverse spinel structure differed little from that of standard, orthorhombic  $\text{NiFe}_2\text{O}_4$ , with a cation distribution difficult for calculation.

The shape and size of the nanoparticles were determined by transmission electron microscopy (TEM) on a JEOL JEM-1011 operated at an accelerating voltage of 100 kV. Prior to particle size determination, the nanopowder was dispersed in ethanol by sonication. The resultant dispersion was applied to a copper grid which had been sequentially coated with Formvar and carbon.

Elemental analysis was carried out on a Philips SEMS 515 scanning electron microscope equipped with an EDAX ECON IV microanalysis system. The detection limit and largest error of determination for the elements present were 0.2 and 2.0%, respectively. The scan area for microanalysis was  $1.0 \times 1.0 \times 5.0 \mu\text{m}$ .

In magnetic studies, we employed a multipurpose cryogenic high-field measurement system [16]. In addition to standard magnetization versus magnetic field measurements, we measured the magnetic susceptibility of the material after cooling in zero field (ZFC) or a low magnetic field (FC). In the ZFC procedure, the sample was cooled to 4 K without applying a magnetic field and measurements were made in a static magnetic field. Next, the temperature was slowly raised and the magnetization was recorded. The FC procedure differed from the ZFC measurements only in that the sample was cooled in a non-zero magnetic field. FC and ZFC curves of magnetically inhomogeneous magnetic materials typically coincide at high temperatures but differ below their blocking temperature,  $T_b$ . Their ZFC curves have a maximum at  $T_b$ , whereas their FC curves usually rise monotonically down to very low temperatures.

## RESULTS AND DISCUSSION

The experimental elemental analysis data for the synthesized powder (table) showed increased iron and oxygen concentrations relative to stoichiometric nickel ferrite ( $\text{NiFe}_2\text{O}_4$ ). The composition of the powder obtained in this study was  $x\text{NiFe}_2\text{O}_4 \cdot y\text{Fe}_2\text{O}_3 \cdot z\text{H}_2\text{O}$  ( $\text{NiFe}_{4.6}\text{O}_{14.8}$ ); that is, the procedure described above yielded nonstoichiometric nickel ferrite. This composition resulted from the fact that the synthesis process was accompanied by partial removal of nickel hydroxide because of its amphoteric nature. Moreover, the synthesized powder probably contained, in addition to iron and nickel hydroxides, the iron compounds  $(\text{C}_{12}\text{H}_{25}\text{SO}_4)_3\text{Fe}$ ,  $(\text{C}_{12}\text{H}_{25}\text{SO}_4)_2\text{Fe}(\text{OH})$ , and  $(\text{C}_{12}\text{H}_{25}\text{SO}_4)\text{Fe}(\text{OH})_2$ . They were difficult to isolate by filtering the precipitate and, most likely, remained in the mixture of nickel and iron hydroxides and in the powder obtained. This is evidenced by the rather high carbon content of the material obtained, which is only attributable to the residual SDS. This type of composite is referred to as "magnetic soap" and was described in detail by Mirgorod et al. [16] and Brown et al. [17].

The XRD pattern of the synthesized powder (Fig. 1) had no sharp peaks, in contrast to diffraction patterns of perfect crystals. The elemental analysis and XRD data for the powder provide conclusive evidence that it con-

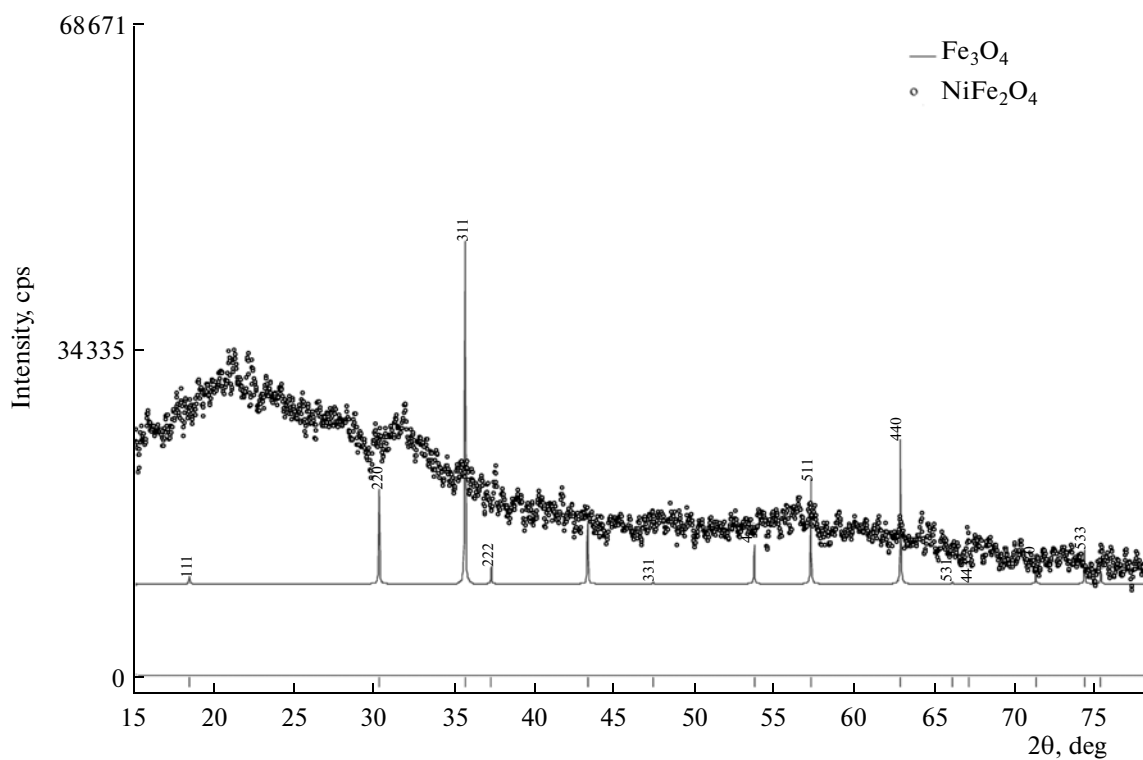


**Fig. 1.** XRD pattern of the synthesized nickel ferrite in comparison with a calculated XRD pattern of  $\text{Fe}_3\text{O}_4$ .

sisted of X-ray amorphous, nonstoichiometric nickel ferrite and a surfactant. Heat treatment at  $600^\circ\text{C}$  caused diffraction peaks from macrocrystalline nickel ferrite to emerge.

The presence of dodecyl sulfates and hydroxyl groups led to the formation of a robust adlayer on the ferrite nanoparticles. The nanoparticles of the synthesized nonstoichiometric nickel ferrite ranged in size

from 2 to 6 nm (Fig. 2a). Heat treatment at  $600^\circ\text{C}$  increased the particle size (Fig. 2b).

Nanoparticles 2–6 nm in size are single-domain [1, 18]. The magnetic moments of all the atoms in the bulk of a domain are parallel to each other, and those of the atoms on its surface are oriented at random. If a bit of information will be carried by a 6-nm particle of the synthesized nickel ferrite instead of a 60- $\mu\text{m}$  domain in

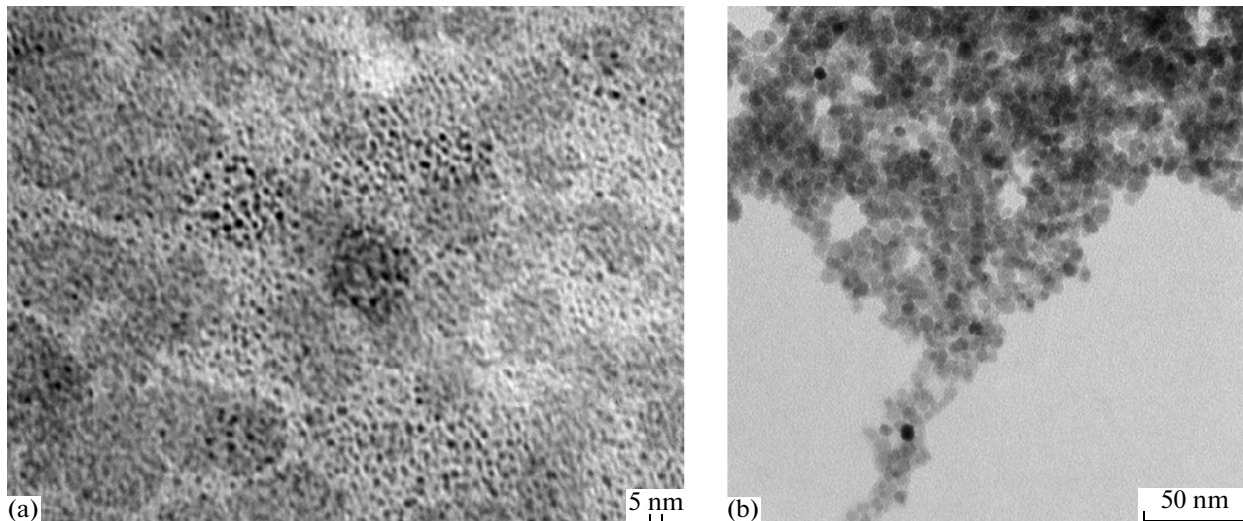


**Fig. 2.** TEM micrographs of (a) as-prepared and (b) heat-treated nickel ferrite nanoparticles.

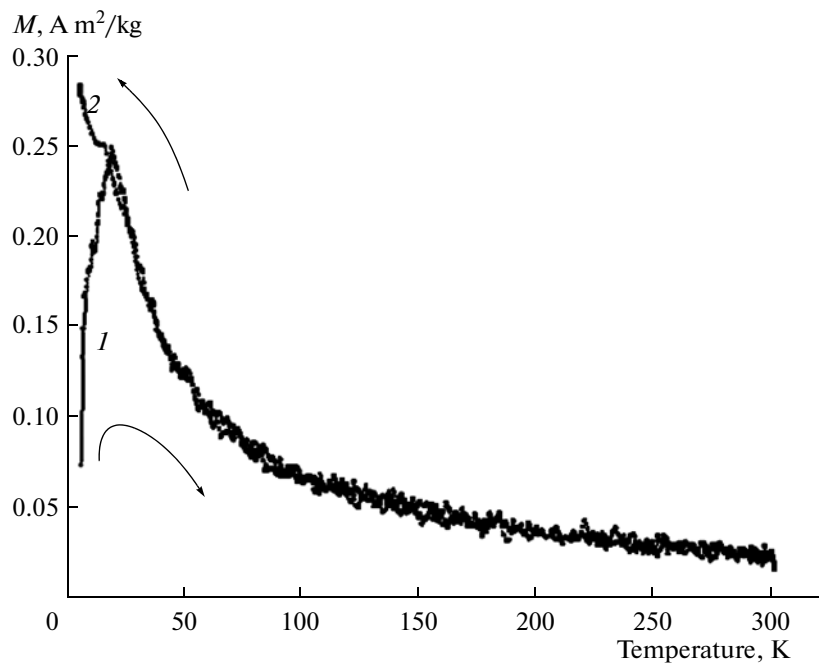


**Fig. 3.** Temperature dependences of specific magnetization for the synthesized nickel ferrite in a magnetic field of 24 kA/m: (1) ZFC, (2) FC.

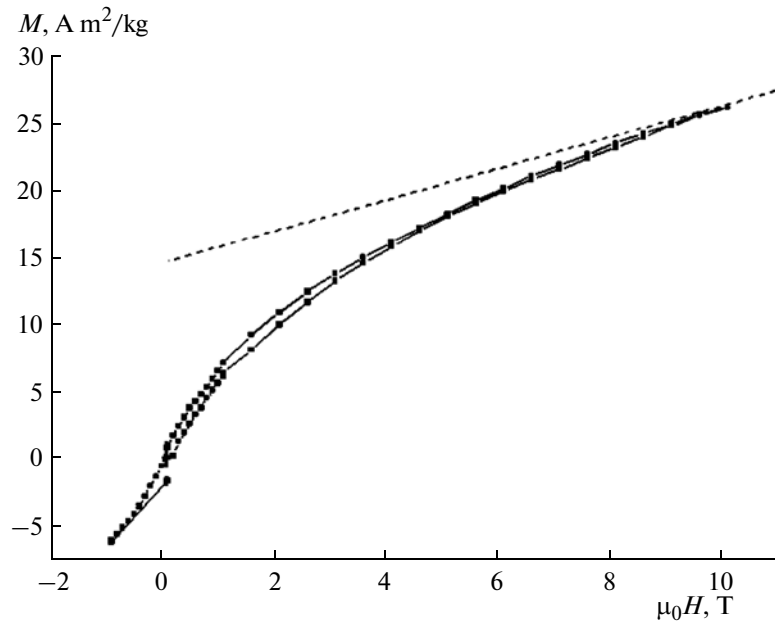


**Fig. 4.** Magnetic field dependence of specific magnetization for the synthesized nickel ferrite at 5 K.

modern disks, the information storage density will be  $10^4$  times higher [18]. For a nanoparticle to carry a bit of information, its magnetization should be reversed by an applied positive field (writing) or negative field (erasure) and should retain its orientation in the absence of a field (storage). Nanoparticles possess such properties up to their blocking temperature. To reverse the magnetization direction, a critical field (coercive force) should be

applied in the opposite direction. The nanomaterials under consideration have a critical field as low as  $0.1 T_c$  (Fig. 3), meaning that even the low magnetic fields around us will cause such nanoparticles to “lose memory.” At temperatures above  $T_b = 25$  K, the synthesized nickel ferrite nanoparticles possess superparamagnetic properties (Fig. 3), which is characteristic of magnetic nanomaterials [1, 19].

The blocking temperature of nanoparticles can be raised through their self-organization. Magnetic dipole–dipole interactions in the nanoparticles will then increase the internal energy of the system. Because of the increase in energy barrier height, the blocking temperature will exceed that of an individual particle and will be given by  $T_b \sim (T_b \sim (KV + E_{\text{dip}})/25k_B)$ . Note that this formula is for the  $T_b$  of a periodic colloidal structure on the substrate surface rather than for the  $T_b$  represented in Fig. 3. Another important characteristic of a magnetic nanomaterial is its specific saturation magnetization. That of the synthesized ferrite nanoparticles is  $15.0 \text{ A m}^2/\text{kg}$  at  $5 \text{ K}$  (Fig. 4), which is slightly below the saturation magnetization of bulk  $\text{NiFe}_2\text{O}_4$  ( $17.6 \text{ A m}^2/\text{kg}$ ) [20]. Magnetite also has such differences:  $50.3$  [21] or  $60.1 \text{ A m}^2/\text{kg}$  [22] against  $92.0 \text{ A m}^2/\text{kg}$ ; that is, in our case the specific saturation magnetization of the nanoparticles is lower than that of bulk magnetic materials.

## CONCLUSIONS

A method has been proposed for the preparation of nanoparticles of nonstoichiometric nickel ferrite with the composition  $x\text{NiFe}_2\text{O}_4 \cdot y\text{Fe}_2\text{O}_3 \cdot z\text{H}_2\text{O}$  in a system of direct sodium dodecyl sulfate micelles using ion flotation. The method can be used in recycling used magnets. The XRD pattern of the material prepared by this method has no strong reflections, in contrast to diffraction patterns of perfect crystals, but heat treatment gives rise to strong reflections, typical of bulk nickel ferrite. The size distribution of the synthesized nanoparticles has a maximum in the range 4 to 6 nm, and they can form periodic island structures. The blocking temperature of the synthesized nanopowder is about  $25 \text{ K}$  and it possesses superparamagnetic properties, with a specific saturation magnetization of  $15 \text{ A m}^2/\text{kg}$  at  $5 \text{ K}$ .

## ACKNOWLEDGMENTS

This work was supported by the RF Ministry of Education and Science through the federal targeted program *The Scientists and Science Educators of Innovative Russia*, project no. P848, R.

## REFERENCES

- Gubin, S.P., Koksharov, Yu.A., Khomutov, G.B., and Yurkov, G.Yu., Magnetic Nanoparticles: Preparation, Structure, and Properties, *Usp. Khim.*, 2005, vol. 74, pp. 539–574.
- Fionov, A.S., Kolesov, V.V., and Yurkov, G.Yu., Polyethylene-Matrix Composites Containing  $\text{NiFe}_2\text{O}_4$  Nanoparticles, *Materialy XX mezhdunarodnoi Krymskoi konferentsii "SVCh-tehnika i telekommunikatsionnye tekhnologii" (KryMiKo 2010)* (Proc. XX Int. Crimean Conf. Microwave Engineering and Telecommunication Technologies, KryMiKo 2010), Sevastopol, 2010, pp. 769–770.
- Singhal, S. and Chandra, K., Cation Distribution and Magnetic Properties in Chromium-Substituted Nickel Ferrites Prepared Using Aerosol Route, *J. Solid State Chem.*, 2007, vol. 180, no. 1, pp. 296–300.
- Shultz, M.D., Calvin, S., Fatouros, P.P., et al., Enhanced Ferrite Nanoparticles As MRI Contrast Agents, *J. Magn. Magn. Mater.*, 2007, vol. 311, no. 1, pp. 464–468.
- Zhao, H., Zheng, Z., Wong, K.W., et al., Fabrication and Electrochemical Performance of Nickel Ferrite Nanoparticles As Anode Material in Lithium Ion Batteries, *Electrochem. Commun.*, 2007, vol. 9, no. 10, pp. 2606–2610.
- Baruwati, B., Guin, D., and Manorama, S.V., Pd on Surface-Modified  $\text{NiFe}_2\text{O}_4$  Nanoparticles: A Magnetically Recoverable Catalyst for Suzuki and Heck Reactions, *Org. Lett.*, 2007, vol. 9, no. 26, pp. 5377–5380.
- Berkowitz, A.E., Lahut, J.A., Jacobs, I.S., et al., Spin Pinning at Ferrite–Organic Interfaces, *Phys. Rev. Lett.*, 1975, vol. 34, pp. 594–597.
- Gopal Reddy, C.V., Manorama, S.V., and Rao, V.J., Semiconducting Gas Sensor for Chlorine Based on Inverse Spinel Nickel Ferrite, *Sens. Actuators, B*, 1999, vol. 55, no. 1, pp. 90–95.
- Satyanarayana, L., Madhusudah Reddy, K., and Manorama, S.V., Nanosized Spinel  $\text{NiFe}_2\text{O}_4$ : A Novel Material for the Detection of Liquefied Petroleum Gas in Air, *Mater. Chem. Phys.*, 2003, vol. 82, no. 1, pp. 21–26.
- Suzuki, T., Nakayama, T., Suzuki, T., et al., Change in Electrical Resistivity of  $\text{NiFe}_2\text{O}_4$  Porous Bulks Caused by Adsorption and Desorption of Alcohols, *Jpn. J. Appl. Phys.*, 2008, vol. 47, pp. 661–663.
- Cote, L.J., Teja, A.S., Wilkinson, A.P., and Zhang, Z.J., Continuous Hydrothermal Synthesis of  $\text{CoFe}_2\text{O}_4$  Nanoparticles, *Fluid Phase Equilib.*, 2003, vol. 210, no. 2, pp. 307–317.
- Chinnasamy, C.N., Narayanasamy, A., Ponpandian, N., et al., Mixed Spinel Structure in Nanocrystalline  $\text{NiFe}_2\text{O}_4$ , *Phys. Rev. B: Condens. Matter Mater. Phys.*, 2001, vol. 63, pp. 184 108–184 113.
- Morr, A.H. and Haneda, K., Magnetic Structure of Small  $\text{NiFe}_2\text{O}_4$  Particles, *J. Appl. Phys.*, 1981, vol. 52, no. 3, pp. 2496–2498.
- Ramalho, M.A.F., Gama, L., Antonio, S.G., et al., X-Ray Diffraction and Mossbauer Spectra of Nickel Ferrite Prepared by Combustion Reaction, *J. Mater. Sci.*, 2007, vol. 42, pp. 3603–3606.
- Doyle, F.M., Ion Flotation—Its Potential for Hydrometallurgical Operations, *Int. J. Miner. Process.*, 2003, vol. 72, nos. 1–4, pp. 387–399.
- Mirgorod, Yu.A., Borshch, N.A., Reutov, A.A., et al., Synthesis of Gadolinium-Based Nanoparticles in a System of Direct Surfactant Micelles and Study of Their Magnetic Properties, *Russ. J. Appl. Chem.*, 2009, vol. 82, no. 8, pp. 1357–1363.
- Brown, P., Bushmelev, A., Butts, C.P., et al., Magnetic Control over Liquid Surface Properties with Respon-

- sive Surfactants, *Angew. Chem., Int. Ed.*, 2012, vol. 51, pp. 1–4.
18. Gubin, S.P., Spichkin, Yu.I., Yurkov, G.Yu., and Tishin, A.M., Nanomaterial for High-Density Magnetic Data Storage, *Russ. J. Inorg. Chem.*, 2002, vol. 47, suppl. 1, pp. 32–67.
19. Yurkov, G.Yu., Gubin, S.P., Pankratov, D.A., et al., Iron(III) Oxide Nanoparticles in a Polyethylene Matrix, *Inorg. Mater.*, 2002, vol. 38, no. 2, pp. 137–145.
20. Bhavikatti, A.M., Kulkarni, S., and Lagashetty, A., Electromagnetic Studies of Nickel Ferrite Synthesized by Microwave Route, *Int. J. Eng. Sci. Technol.*, 2011, vol. 3, no. 1, pp. 687–695.
21. Liu, Z.L., Lin, Y.J., Yao, K.L., et al., Synthesis and Magnetic Properties of  $\text{Fe}_3\text{O}_4$  Nanoparticles, *J. Mater. Synth. Proc.*, 2002, vol. 10, pp. 83–87.
22. Zhao, S.-Y., Lee, D.K., Kim, C.W., et al., Synthesis of Magnetic Nanoparticles of  $\text{Fe}_3\text{O}_4$  and  $\text{CoFe}_2\text{O}_4$  and Their Surface Modification by Surfactant Adsorption, *Bull. Korean Chem. Soc.*, 2006, vol. 27, no. 2, pp. 237–242.